ISSN 2314-5609
Nuclear Sciences Scientific Journal
5, 69 -90
2016
http://www.ssnma.com

Nuclear Materials Authority
P.O.Box 530 Maadi, Cairo, Egypt

GEOLOGY AND RADIOACTIVITY OF PERALUMINOUS GRANITE AND ASSOCIATED PEGMATITE HOSTING MAGNETITE MINERALIZATION AT UM REGEBA AREA, SOUTHEASTERN DESERT, EGYPT

FARRAGE M. KHALEAL and MOHAMED S. KAMAR
Nuclear Materials Authority, P.O. Box 530 El-Maadi, Cairo, Egypt.

ABSTRACT

The study area represents the southeastern part of Wadi El-Gemal-Hafafit culmination in the south Eastern Desert of Egypt. Magnetite mineralization occurs in Wadi El-Gemal area in many localities, Um Regeba area is the case study.

Petrographically, the studied peraluminous granites (PG) are medium- to coarse-grained and mainly composed of plagioclase (An_{5-10}), K-feldspar, quartz, biotite and muscovite. Sericite and chlorite are secondary minerals, while allanite and zircon are the common accessories. The peraluminous pegmatites (PP) are coarse-grained and composed essentially of K-feldspar, quartz, plagioclase (An_{6-10}), muscovite and biotite. Titanite, allanite, zircon and magnetite are common accessories.

Geochemically, the studied peraluminous granites and peraluminous pegmatites are monzogranite and syeno- to alkali feldspar granite respectively. They have peraluminous character, calc alkaline and alkaline affinities respectively, emplaced in within plate setting, crystallized under water–vapor pressure (2-3 Kb), temperature from 760° to 800° C, pertaining to the I-type granite originated by highly differentiated magma generated from upper mantle contaminated with some crustal materials.

Magnetite usually occurs as small lumps, concentrated by to accumulation in magmatic segregations that developed in response to fractional crystallization. Magnetite showed lamellar intergrowth with ilmenite. The latter can be seen with a hand lens in most magnetite samples. The magnetite of Um Regeba area represents a late stage magmatic product. From the microprobe results, magnetite is characterized by high content of SiO_2, Al_2O_3, CoO and Cr_2O_3, whereas ilmenite is characterized by high content of MnO and ZnO. The average eU content in the peraluminous granites is 1.96 ppm, while it reaches 5.65 ppm for eTh. The average eU content in the peraluminous pegmatites is 9.12 ppm, while the average eTh content is 21.76 ppm.

INTRODUCTION

Peraluminous granitic segregations are commonly associated with regionally metamorphosed terrains (Clemens and Wall, 1981), Debon et. al. (1986), Inger and Harris (1993). Numerous mechanisms have been proposed to explain the derivation of these segregations from the metamorphosed host rock. Partial melting of metapelites is still the most widely accepted model for the generation of these peraluminous granites (Holtez and Barbey, 1991). The breakdown of the hydrous silicates in these pelites (such as muscovite and biotite minerals) produces most of the water required for this partial melting process (Fyfe, 1969).

Four principal mechanisms for the formation of peraluminous granites have previously been advocated (Mohamed and Hassanen, 1997): (1) the peraluminous granite is directly linked to peraluminous source rocks, (2) the peraluminous granite may, at least in part, be the result of reaction with host rocks, (3) the peraluminous granite has been derived from meta-aluminous magmas by fractional crystallization and (4) the peraluminous granite is at least in part if not wholly, the result of interaction between late stage magmas or subsolidus rocks and hydrothermal fluids.

In Egypt, the peraluminous granites represent phases of orogenic to late orogenic. Their quartz veins are rich in -Mo, Sn, W, U, Nb and -Ta mineralization within the granitic rocks (Takla and Nowier, 1980).

Most of the pegmatites are usually associated with granitoid rocks, but little is incorporated with mafic-ultramafic rocks. The pegmatites can be roughly categorized according to their alkali concentration ratios, as follows: primitive pegmatites, intermediate pegmatites and evolved pegmatite (Jolliff et al., 1992).

Granitic pegmatite magma is peraluminous and characterized by enrichment in volatiles such as F, P, B and/or H_2O. It has been demonstrated that such volatiles have a significant influence on the evolution of the pegmatite magma, the temperatures of the solidus and liquids of the magma, the viscosity of the silicate melt, the crystallization sequence of minerals and also on the partition behavior of trace elements between fluid and melt (Černý and Meintzer 1985; Webster and Rebbert, 1998; London, 1987; Ding-well et al., 1998, Bai and Van Groas, 1999, Keppler and Wyllie, 1991 and Keppler, 1993).

Magnetite occurs in the peraluminous pegmatites and granites in many localities of W. El Gemal area, especially in El Mokhattata area. The Um Regeba area is the case study for this mineralization and this is the first record of magnetite mineralization in the area. Magnetite forms under a wide variety of conditions, crystallizing at high temperature from silicate, sulfide and carbonatite magmas or it can precipitate at lower temperatures from hydrothermal fluids. These different conditions may lead to distinctive trace element signatures for the magnetite. It is possible to use the trace element signature of magnetite as petrogenetic and provenance indicators (Dare et al., 2013).

The main target of this work is to study the magnetite mineralization as well as the hosting peraluminous granites and pegmatites of Um Regeba area geologically, geochemically, mineralogically and radiometrically.

METHODS OF STUDY

Detailed petrographic examination was carried out to study the mineral constituents and textural patterns of the rock. Fourteen samples (14) were chemically analyzed for major and trace elements from the peraluminous granites (9 samples) and peraluminous pegmatites (5 samples). The heavy minerals were separated using heavy liquid (bromoform), followed by magnetic separation using Frantz Isodynamic Separator. The obtained fractions magnetic and non-magnetic were investigated under binocular microscope. All analyses were carried out in the Laboratories of Nuclear Materials Authority (NMA), Cairo, Egypt. Some individual grains of magnetite were picked and analyzed by X-ray diffraction (XRD) method (in the Laboratories of NMA), and the backscattered electron images were performed at the Microscopy and Microanalyses Facility, University of New Brunswick (UNB), Fredericton, New Brunswick, Canada (model JEOL 6400 SEM).

GEOLOGIC SETTING

The studied area is located about 80 km SW of Marsa Alam city on the Red Sea Coast (Fig. 1), between lat. 24° 31' 40" - 24° 38' 20" N and long. 34° 37' 30"- 34° 50' E. It represents the southeastern most part of the Nugrus-Hafafit culmination in the south Eastern Desert (Figs. 1& 2).

The exposed rocks were classified (Greiling, 1990) into the following litho-tectonic units: 1) psammitic gneiss, mostly quartz rich meta-psammites, meta-conglomerates and subordinate meta-pelites; 2) Migif-Hafafit gneisses and associated ultramafic and calc-alkaline igneous assemblages, granitoids and metasediments, generally medium metamorphic grade; 3) white gneissic granodiorite, trondhjemite, tonalite complex; 4) peraluminous granites and peraluminous pegmatites bearing magnetite (the present study); 5) late-orogenic granitoids (microgranite, felsite and aplite) ,(Fig. 2).

The Um Regeba peraluminous granites are characterized by white colour, medium- to coarse-grained and occasionally pegmatitic. The former were emplaced into the older rocks in NNW-SSE trend (striking 350°) (Figs. 3 and 4) close to the major Nugrus thrust. The peraluminous granites contain - in parts - xenoliths from the older rocks; these enclaves form lenses usually exceeding 10 cm in length. The peraluminous pegmatites occur as dyke–like bodies of variable

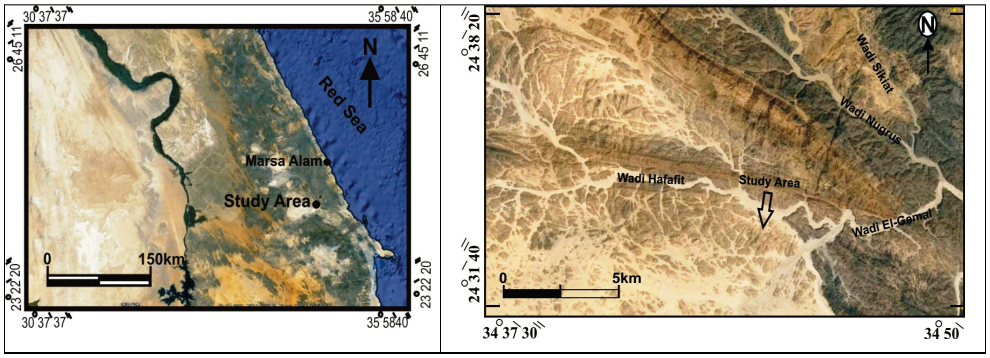

Fig. 1: Landsat image showing the location of the Um Regeba area, SED, Egypt

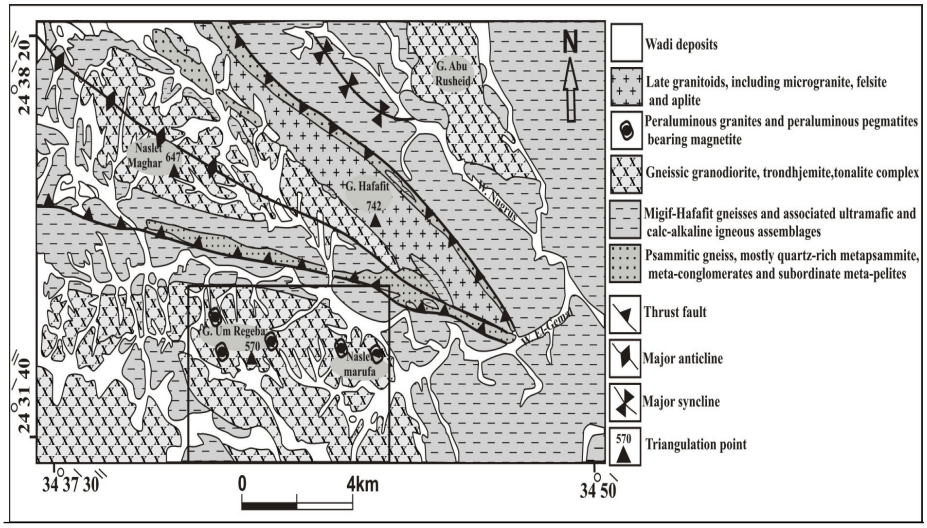

Fig. 2: Geological map of Wadi El Gemal area, the rectangular part is the Um Regeba area, SED, Egypt (Modified after Greiling, 1990)

dimensions intruding the granodiorite of the studied area with sharp contact (Fig. 3). They vary from few centimeters to few meters in width and length, and mostly concordant with the common NW-SE trend of the enclosing granites as well as the other country rocks all - over the area (Fig. 4). The magnetite mineralization is associated with the peraluminous pegmatites (Figs. 5 and 6).

PETROGRAPHY

Peraluminous Granites

The peraluminous granites are medium- to coarse-grained, mainly composed of plagioclase, K-feldspar, quartz, biotite and muscovite. Sericite and chlorite are the secondary minerals, while allanite and zircon are the common accessories.

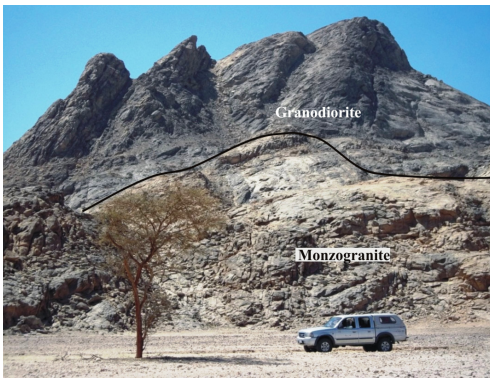

Fig. 3: General view of peraluminous granites (monzogranite) in G. Um Regeba area, SED, Egypt, Looking NNW

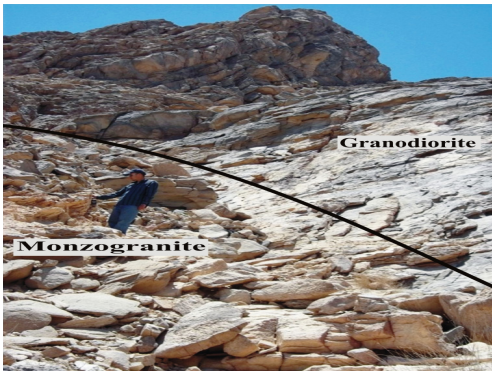

Fig. 4: The sharp contact between peraluminous granites (monzogranite) and granodiorite in G. Um Regeba area, SED, Egypt, Looking NNW

Fig. 5: Peraluminous pegmatites bearing magnetite, G. Um Regeba area, SED, Egypt, Looking NNW


Fig. 6: Overview showing individual magnetite crystals, G. Um Regeba area, SED, Egypt

Plagioclase is presented by albite (An_{5-10}), which occurs as twinned subhedral to euhedral crystals exhibiting wide range of grain sizes, enclosing sometimes fine crystals of quartz (Fig. 7). The former shows varied degrees of alteration to clay minerals (Fig. 8). Sometimes, it shows corrosion boundaries with quartz (Fig. 9). ***K-feldspars*** are represented by microcline and microcline microperthite. Microcline microperthite is observed in subordinate amount as anhedral to subhedral crystal showing the characteristic cross-hatching or tartan pattern (Fig. 10), as a

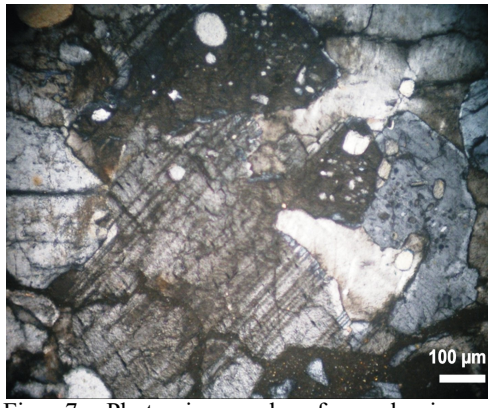

Fig. 7: Photomicrograph of peraluminous granites showing plagioclase with albite twinning enclosing fine crystals of quartz, XPL

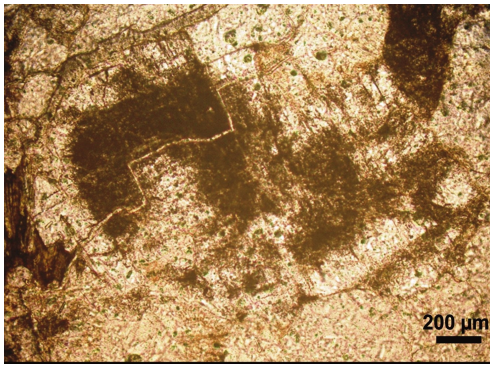

Fig. 8 : Photomicrograph of peraluminous granites showing plagioclase altered to clay minerals, XPL

Fig. 9: Photomicrograph of peraluminous granites showing plagioclase corroded by quartz, XPL

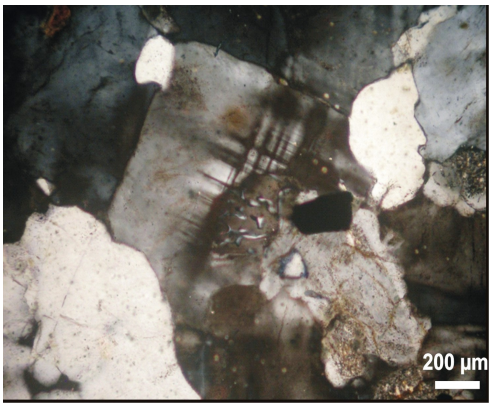

Fig. 10: Photomicrograph of peraluminous granites showing microcline crystal with myrmikitic texture, XPL

result of albite and pericline twins' combination (Deer et. al., 1992). Myrmekitic texture is occasionally present due to the replacement of plagioclase by K-feldspar (Fig. 11). ***Quartz*** occurs as subhedral to anhedral crystals interstitial between the feldspar crystals. Drop like inclusions of quartz are frequently poikilitically enclosed in the feldspar crystals. ***Biotite*** is the dominant mafic mineral, occurs as euhedral to subhedral crystals. It occurs as brown colour flakes (Fig. 12) variably altered to chlorite. **Muscovite** occurs as euhedral to subhedral colourless flakes. ***Allanite*** occurs as brown euhedral yellowish crystals associated with zircon and iron oxides. ***Zircon*** occurs as euhedral to subhedral prismatic crystals, associated with quartz and iron oxides.

Peraluminous Pegmatites

The pegmatite pockets are composed essentially of ***K-feldspar*** which is mostly represented by orthoclase. Orthoclase occurs as euhedral to subhedral crystals showing simple twinning and occasionally kaolinized. ***Quartz*** occurs as subhedral to anhedral crystals, some crystals show undulose extinction and irregular boundaries. ***Plagioclase*** is acidic in composition (An_{6-10}) exists as euhedral to subheral crystals. It exhibits albite and Carlsbad twinning and occasionally antiperthitic.

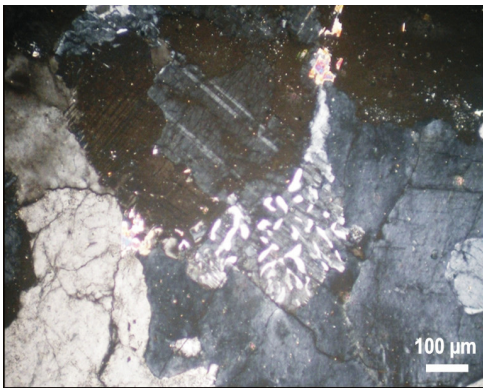

Fig. 11: Photomicrograph of peraluminous granites showing myrmikitic texture, XPL

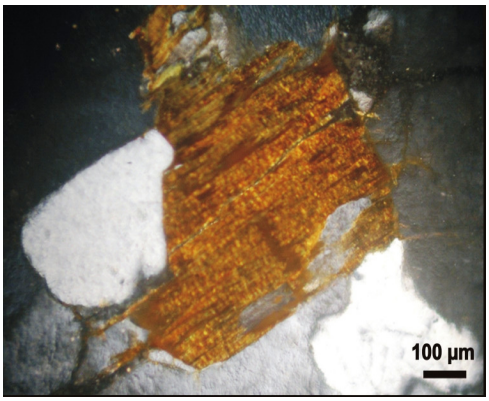

Fig. 12: Photomicrograph of peraluminous granites showing brown flake of biotite, XPL

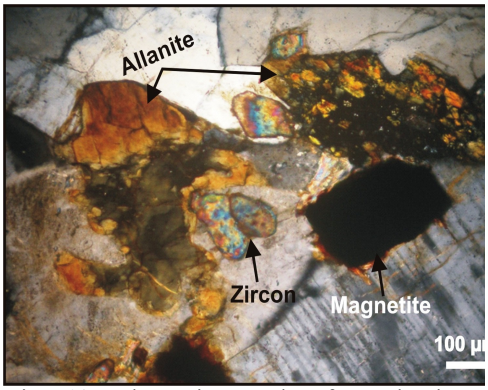

Fig. 13: Photomicrograph of peraluminous pegmatites showing association of zircon, allanite and magnetite, XPL

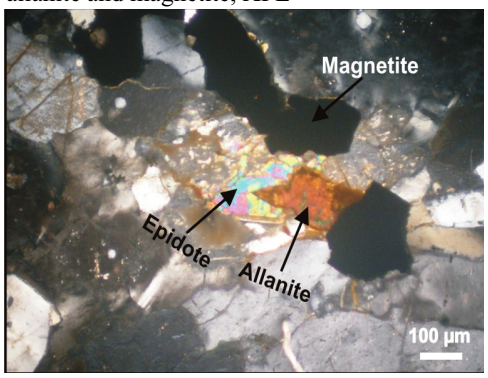

Fig. 14: Photomicrograph of peraluminous pegmatites showing alteration of epidote to allanite and association with magnetite, XPL

Sericitization and kaolinization are encountered. ***Muscovite*** forms subhedral to anhedral flakey crystals, sometimes interstitially filled the space between the major constituents. ***Biotite*** occurs as subhedral flakey crystals stained with iron oxides. ***Zircon*** occurs as euhedral to subhedral prismatic crystals, associated with quartz, allanite and iron oxides (Fig. 13). ***Allanite*** occurs as euhedral yellowish brown crystals associated with zircon and iron oxides, and sometimes result from the alteration of epidote (Fig. 14). ***Titanite*** forms subhedral to anhedral rhombic crystals, associated with biotite. ***Magnetite*** occurs as subhedral to anhedral crystals usually associated with the mafic constituents.

GEOCHEMISTRY

The data of chemical analyses (major oxides, trace elements and normative values) are given in Table (1). The general characteristics of the granitic rocks depend on the behavior and distribution of the major and trace elements. The average chemical composition of the studied peraluminous granites and peraluminous pegmatites when compared with Group II the younger granites of the Eastern Desert (Greenberg, 1981). They show increasing in Al_2O_3, MgO, CaO (PG), Na_2O and P_2O_5 decreasing in SiO_2, TiO_2, Fe_2O_3, CaO

Table 1: The major oxides, trace elements analyses and normative values of the studied peraluminous granites and peralumious pegmatites of G. Um Regeba, SED, Egypt

Oxides %	Peraluminous granites									Peraluminous pegmatites				
	1	2	3	4	5	6	7	8	9	10	11	12	13	14
SiO_2	74.2	73.88	74.61	73.62	73.1	74.95	73.62	73.1	74.9	74.10	74.2	73.8	74.5	74.8
TiO_2	0.12	0.03	0.01	0.05	0.06	0.05	0.04	0.04	0.05	0.05	0.04	0.06	0.03	0.02
Al_2O_3	14.1	15.2	13.87	13.82	13.67	14.22	13.88	13.90	14.1	13.6	13.5	13.8	13.10	12.80
FeO	0.39	0.33	0.51	0.3	0.34	0.33	0.25	0.33	0.44	0.30	0.25	0.30	0.20	0.10
Fe_2O_3	0.65	0.75	0.98	0.82	0.96	0.88	0.96	0.95	0.97	0.60	0.50	0.70	0.40	0.30
MnO	0.01	0.06	0.05	0.08	0.07	0.02	0.08	0.05	0.01	0.07	0.06	0.08	0.05	0.04
MgO	0.35	0.75	0.39	0.77	1.03	0.42	1.09	1.27	0.35	0.08	0.35	0.09	0.06	0.04
CaO	1.45	1.12	0.58	1.1	1.25	1.42	1.22	1.25	1.33	0.40	0.07	0.50	0.30	0.20
Na_2O	4	4.01	4.25	3.95	4	4.11	4	3.91	3.87	4.15	4.22	4.10	4.30	4.40
K_2O	3.93	3.83	3.89	3.85	3.98	3.92	4	3.86	3.67	4.30	4.35	4.20	4.50	4.60
P_2O_5	0.12	0.1	0.02	0.04	0.12	0.09	0.1	1.09	0.06	0.02	0.03	0.02	0.01	0.01
L.O.I	0.52	0.78	0.55	0.62	0.48	0.36	0.49	0.48	0.5	0.70	0.80	0.60	0.80	0.75
Total	99.84	100.8	99.71	99.02	99.06	100.7	99.73	100.2	100.2	98.37	98.37	98.25	98.25	98.06
Fe_2O_3/FeO	1.67	2.27	1.92	2.73	2.82	2.67	3.84	2.88	2.20	2.0	2.0	2.33	2.0	3.0
Na_2O/K_2O	1.02	1.05	1.09	1.03	1.005	1.05	1.0	1.01	1.05	0.97	0.97	0.98	0.96	0.96
CIPW- Normative values														
O	32.82	32.62	33.45	33.08	31.15	32.49	31.32	31.11	35.24	33.34	33.20	33.53	32.38	32.03
Or	23.40	22.64	23.20	23.16	23.88	23.09	23.84	22.89	21.76	26.04	26.37	25.44	27.31	27.96
Ab	34.04	33.87	36.22	33.95	34.29	34.59	34.07	33.13	32.79	35.91	36.55	35.49	37.29	38.22
An	6.54	4.97	2.79	5.31	5.58	6.49	5.51	6.22	6.27	1.91	0.18	2.42	1.47	0.96
C	0.88	2.62	1.66	1.25	0.76	0.81	0.96	1.0	1.46	1.46	1.82	1.67	0.63	0.23
Hv(en)	0.88	1.87	0.98	1.96	2.61	1.05	2.75	3.18	0.88	0.20	0.90	0.23	0.15	0.10
Hv(fs)	0	0.05	0.20	0	0	0	0	0	0	0.11	0.09	0.02	0.08	0
Mt	0.95	1.09	1.43	0.87	1.17	0.98	0.96	1.11	1.31	0.89	0.74	1.04	0.60	0.41
He	0	0	0	0.23	0.17	0.20	0.31	0.18	0.07	0	0	0	0	0
Il	0.23	0.06	0.02	0.10	0.12	0.09	0.08	0.08	0.10	0.10	0.08	0.12	0.06	0.40
Ap	0.26	0.22	0.04	0.09	0.27	0.20	0.22	0	0.13	0.04	0.07	0.04	0.02	0.02
Trace elements (ppm)														
Zn	66	34	23	29	46	18	18	26	59	20	18	25	15	12
Zr	406	220	135	355	239	235	297	227	396	430	460	410	465	475
Rb	75	101	110	101	154	93	107	104	108	155	185	145	190	195
Y	180	99	57	153	105	102	126	97	176	190	201	180	215	220
Ba	385	171	128	218	267	119	134	134	329	220	190	240	185	180
Pb	9	15	14	18	15	15	16	18	10	8	6	10	5	5
Sr	19	10	6	17	11	11	14	11	18	10	8	12	6	6
Ga	9	8	9	12	10	9	10	14	10	8	8	10	6	6
Nb	71	39	23	63	42	42	52	39	70	85	95	75	100	105
Ba/Rb	5.13	1.69	1.16	2.16	0.77	1.28	1.25	1.29	3.05	1.42	1.03	1.66	0.97	0.92
K/Rb	434.9	314.7	293.5	316.4	214.5	349.9	310.3	308.1	282.0	230.2	195.1	240.4	196.6	195.8

(PP) and K_2O. The average chemical composition of the studied peraluminous granites and peraluminous pegmatites show increasing in SiO_2, Na_2O, MnO (PP), K_2O (PP) and P_2O_5 (PG) and decreasing in TiO_2, Al_2O_3, Fe_2O_3, FeO, MnO (PG), MgO (PP), CaO, K_2O (PG) and P_2O_5 (PP) when compared with average of world granites (Le Maitre, 1976). When compared with G. Nasb Aluba (Saleh, 1992), they show increasing in SiO_2, MgO (PG) and Na_2O and decreasing in TiO_2, Al_2O_3, FeO, CaO, MgO (PP) K_2O and P_2O_5. When compared with the muscovite granite at Sikait I (Mahmoud, 2009), they show increasing TiO_2, Al_2O_3 (PG), MnO (PP), MgO (PG), CaO (PG), K_2O, Na_2O and P_2O_5 and decreasing in SiO_2, Al_2O_3 (PP), MnO (PG), MgO (PP), CaO (PP), FeO. When compared with granitic rocks of Egyptian granite (Aly and Moustafa, 1984), they show increasing SiO_2, Al_2O_3 (PG), MgO, MnO (PP), Na_2O, K_2O (PP) and P_2O_5 (PG) and decreasing in TiO_2, Fe_2O_3, FeO, MnO, K_2O (PG) and P_2O_5 (PP). It is nearly compatible with the average chemical composition of Egyptian granites of Aly and Moustafa, 1984, (Table 2). On the Ab-An-Or ternary diagram (O'Connor, 1965), the studied peraluminous granites and peraluminous pegmatites lie in granite field (Fig. 15). On the R_1-R_2 discrimination diagram of De La-Roche et al. (1980), the peraluminous granites fall in the monzogranite field (Fig. 16)

(one sample lies in the syenogranite field), while the peraluminous pegmatites plot in syeno- to alkali feldspar granite. The studied peraluminous granites and peraluminous pegmatites have peraluminous characters according to the alumina saturation of Clarke (1981) on Shand's index diagram (Fig. 17). On the discrimination plot of Sylvester (1989) the studied peraluminous granites lie in the calc-alkaline, (one sample lie in the alkaline and highly fractionated calc-alkaline field), on the other hand the peraluminous pegmatites lie in the alkaline and highly fractionated calc alkaline (Fig.18).

Table 2: Comparison between the average chemical compositions of the studied peraluminous granites and some Egyptian and Worldwide granites

Major Oxides	1	2	3	4	5	6	7
SiO_2	73.99	74.28	74.80	71.3	70.82	76.76	73.2
TiO_2	0.05	0.04	0.15	0.31	0.29	0.02	0.22
Al_2O_3	14.08	13.36	12.80	14.3	14.17	13.50	13.7
Fe_2O_3	0.88	0.50	1.09	1.2	n. d.	n.d.	1.1
FeO	0.36	0.23	n. d.	1.64	1.71	0.40	0.97
MnO	0.04	0.06	n. d.	0.05	0.04	0.04	0.05
MgO	0.71	0.124	0.11	0.71	0.45	0.39	0.46
CaO	1.19	0.294	0.57	1.84	2.46	0.93	1.19
Na_2O	4.01	4.23	3.99	3.68	3.86	3.59	3.84
K_2O	3.88	4.39	4.62	4.1	4.46	3.82	4.28
P_2O5	0.19	0.018	0.05	0.12	1.69	0.01	0.11

n. d. : not detected.
1 : Granites of the Um Regeba area, South Eastern Desert.
2: Pegmatites of the Um Regeba area, South Eastern Desert.
3 : Group II younger granites of Eastern Desert (Greenberg, 1981).
4 : Average of World granites (Le Maitre, 1976).
5 : Average of granite in G. Nasb Aluba (Saleh, 1992).
6: Average of the muscovite granite of Sikiait I, South Eastern Desert (Mahmoud, 2009)
7: Average of Egyptian granite (Aly and Moustafa, 1984)

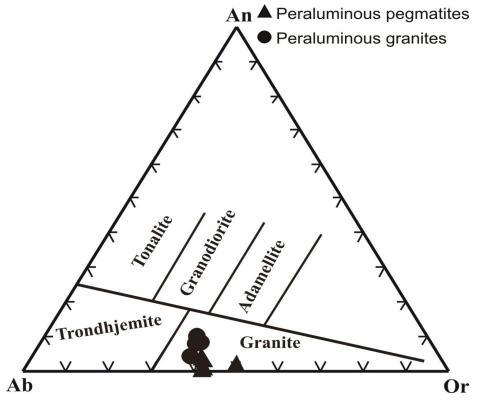

Fig. 15: Ab-An-Or ternary diagram (O'Connor, 1965) for the studied peraluminous granites and peraluminous pegmatites

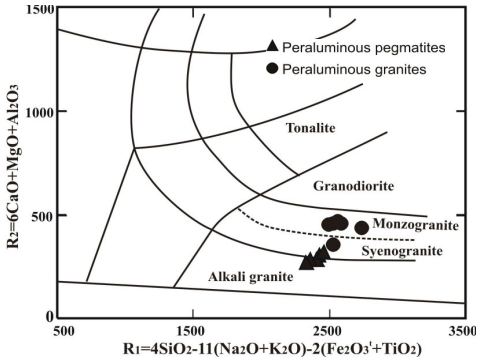

Fig. 16: R_1-R_2 diagram for the studied peraluminous granites and peraluminous pegmatites, After De La Roche et al. (1980)

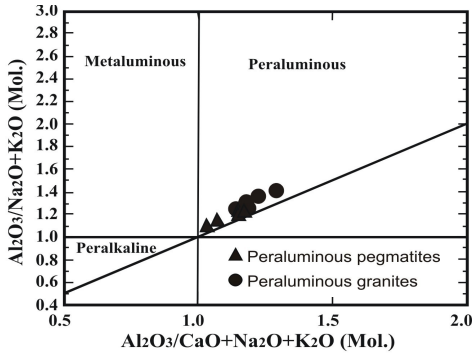

Fig. 17: Shand's index diagram for the studied peraluminous granites and peraluminous pegmatites, After Clarke (1981)

The studied peraluminous granites and peraluminous pegmatites lie in the I-type granite of Chapell and White (1974) (Fig. 19). On Pearce et al. (1984) discrimination diagram (Fig. 20), the studied peraluminous granites and peraluminous pegmatites lie in the within plate granite field. The studied peraluminous granites and peraluminous pegmatites are restricted to the syn-collision field (Fig. 21) after Batchelor and Bowden (1985). The Ab-Qz-Or normative ternary diagrams (Figs. 22&23)

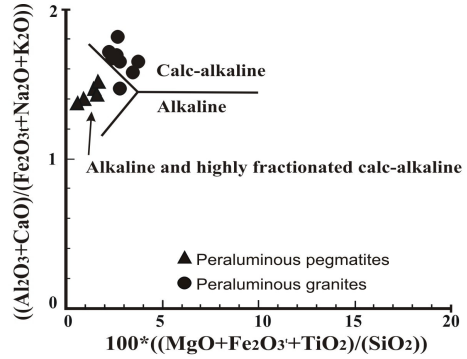

Fig. 18: Major oxides discrimination of granite for the studied peraluminous granites and peraluminous pegmatites, After Sylvester (1989)

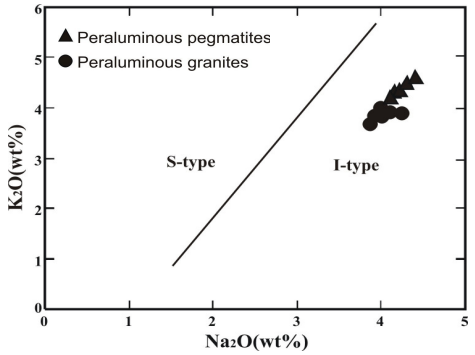

Fig. 19: K_2O vs. Na_2O diagram for I-type and S-type granites for the studied peraluminous granites and peraluminous pegmatites, Fields After Chapell and White (1974)

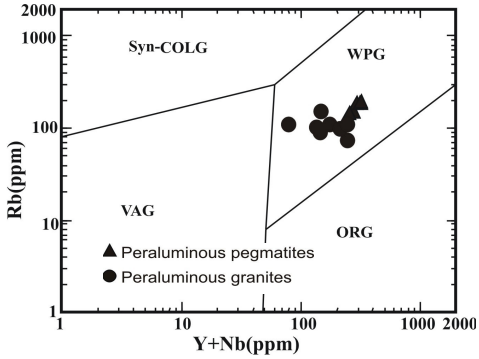

Fig. 20: Rb-(Y+Nb) diagram for the studied peraluminous granites and peraluminous pegmatites(After pearce et al. ,1984)

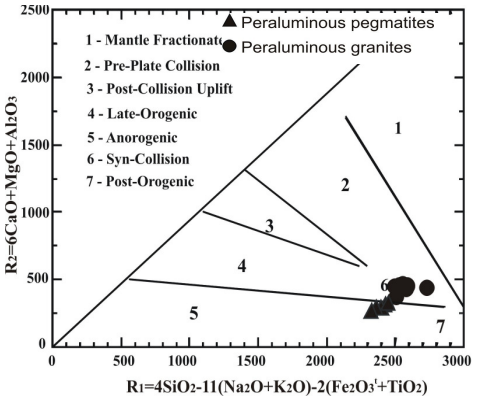

Fig. 21: Multicationic variations diagram for the studied peraluminous granites and peraluminous pegmatites, De La Roch et al. (1980), fields of tectonic setting after Batchelor and Bowden (1985)

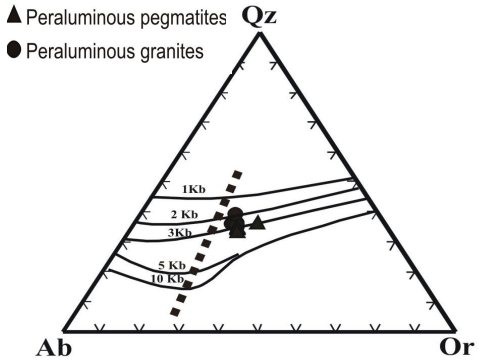

Fig. 22: Ab-Qz-Or diagram for the studied peraluminous granites and peraluminous pegmatites. The dashed lines represent the minimum melting points in the granite system at different water-vapor pressure. 1, 2 &3 kb after Tuttle and Bowen (1958), 5&10 kb after Luth et al. (1964)

reveal that the studied peraluminous granites and peraluminous pegmatites have water-vapor pressure (2 to 3 kb) and temperature from 760° to 800° C suggesting a formation at moderate levels in the crust. The Fe_2O_3/FeO ratio varies from1.67 to 3.84 more than 1 (Table 1), suggesting that the rock originated under higher oxidizing condition (Shalaby, 1995 and Ali et al., 1998). The Rb/Zr ratio vs. SiO_2

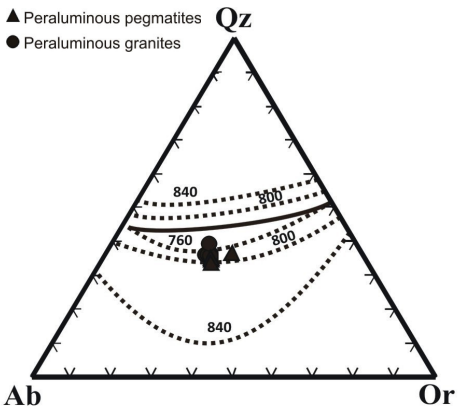

Fig. 23: Ab-Qz-Or diagram for the studied peraluminous granites and peraluminous pegmatites, After Luth et al. (1964)

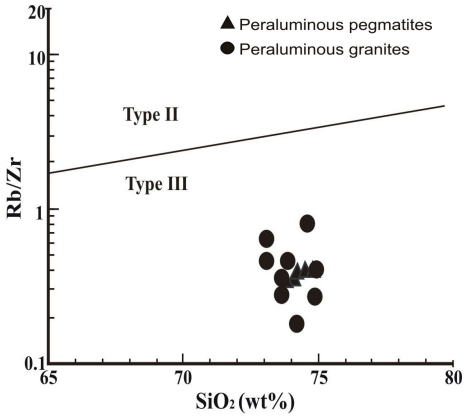

Fig. 24: Rb/Zr vs. SiO_2 discrimination diagram, After Harries et al. (1986)

(Harries et al., 1986) (Fig. 24), reveals that the studied peraluminous granites and peraluminous pegmatites lie in the field of type III. It indicates that the studied peraluminous granites melts could be originated in the the LILE- enriched mantle wedge and contaminated by crustal melts.

The Rb versus K/Rb diagram (Fig. 25) for the studied peraluminous granites and peraluminous pegmatites, show that the Rb tend to be enriched relative to the K in the strongly differentiated granites (Imeokparia, 1981) and the K/Rb ratio ranges from 214.54 to 434.99 for the peraluminous granites while it is 195.10 to 240.40 for the peraluminous pegmatites. The ratio of Ba/Rb decrease with magmatic differentiation due to the crystallization of the feldspar (Fig. 26). In the studied peraluminous granites and peraluminous pegmatites, the Ba/Rb ratio ranges between 0.77 to 5.13 with an average of 1.98, and from 0.92 to 1.66 with an average of 1.20, indicating derivation from mantle origin contaminated with crustal materials.

Spiderdigram of normalized elements data of peraluminous granites and peraluminous pegmatites relative to Chondrite of Sun and McDonough (1989) (Fig. 27), illustrating

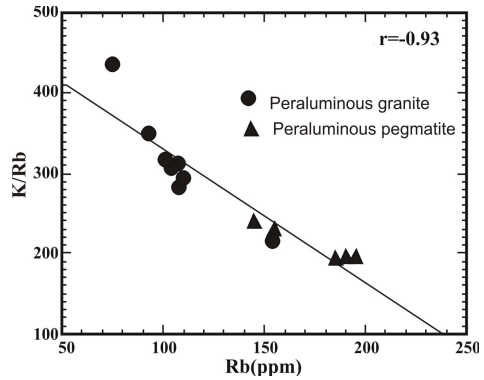

Fig. 25: K/Rb vs. Rb diagram for the studied peraluminous granites and peraluminous pegmatites

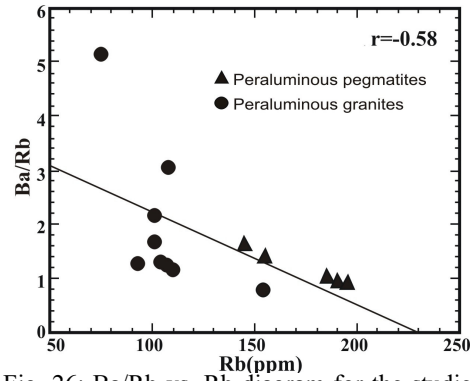

Fig. 26: Ba/Rb vs. Rb diagram for the studied peraluminous granites and peraluminous pegmatites

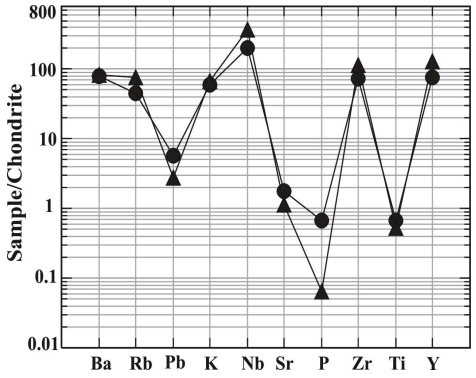

Fig. 27: Spiderdiagram of normalized element data of peraluminous granites and peraluminous pegmatites. Normalized values refer to Chondrite of Sun and McDonough (1989)

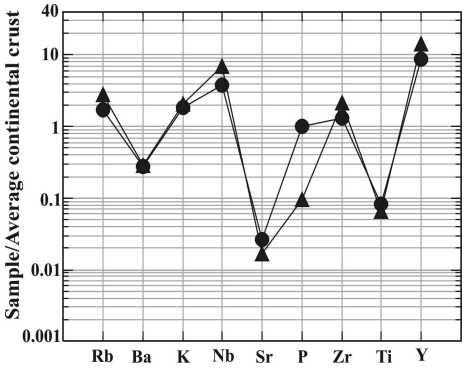

Fig. 28: Spiderdiagram of normalized element data of peraluminous granites and peraluminous pegmatites. Normalized values refer to average continental crust of Weaver and Tarney (1984)

the enrichment of Ba, Rb, Pb, K, Nb, Zr, Y and depletion of P and Ti, while Sr distribute around the unity. Spiderdigram of normalized elements data of peraluminous granites and peraluminous pegmatites relative to average continental crust of (Weaver and Tarney, 1984) are given in (Fig. 28). They show enrichment of Rb, K, Y, Nb and Zr, and depletion of Ba, Sr, Ti and P (PP), while P (PG) distribute around the unity.

MINERALOGY

Detailed microscopic investigations supported by X-ray diffraction (XRD) and ESEM techniques were used for the identification of the accessory and heavy minerals from the peraluminous pegmatites samples. Based on X-ray patterns and ESEM techniques, the minerals can be classified according to their anion into the following groups:

Silicate Minerals

Zircon ($ZrSiO_4$)

Zircon crystal showed different forms such as bipyramids, short prisms with brown or honey brown colour, may exists as normal or metamict. It is iso-structural with xenotime. It is confirmed by XRD-technique (Figs. 29-31).

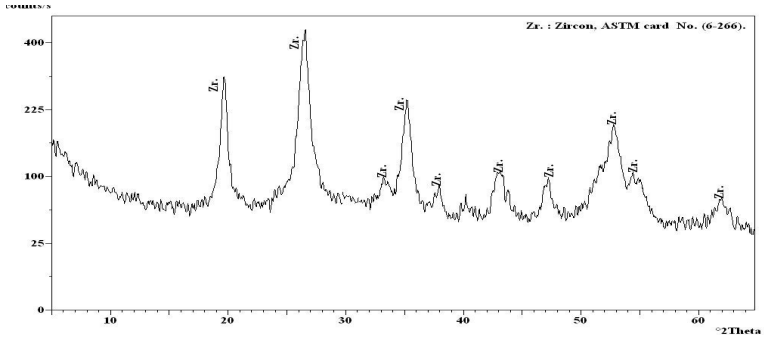

Fig. 29: X-ray diffraction pattern of zircon in the studied peraluminous pegmatites

Phlogopite [K (Mg,Fe)$_3$AlSi$_3$O$_{10}$(F,OH)$_2$]

It is reddish brown in colour and was detected by XRD-technique (Fig. 30).

Phosphate minerals [Xenotime (YPO_4)]

Xenotime is a widespread and important rare earth bearing mineral, where Y can substitute by U, Ca and Si. It is considered as iso-structural mineral with zircon. Khomyakov (1970) has considered the potential of coexisting monazite and xenotime as a geotherometer. El-Kammar et al. (1997a) considered xenotime is a good host for the rare earth elements, where it concentrates the heavy rare earths. This mineral is confirmed by XRD-technique (Fig. 31).

Oxide Minerals

Magnetite (Fe_3O_4)

Magnetite is a common, highly magnetic, black opaque mineral with a metallic luster and high specific gravity (4.9–5.2). It is one of the important iron ores and is a common constituent of igneous and metamorphic rocks. Due to its black colour, surface chemistry and strong magnetic property, it has found a great number of applications in industry. Magnetite crystals reach 2cm in size (Fig. 6). It is found as inclusions in the essential minerals or as secondary minerals filling cracks and cleavage planes. It is confirmed by XRD-technique (Fig. 32) and by ESEM techniques (Fig. 33) and contains

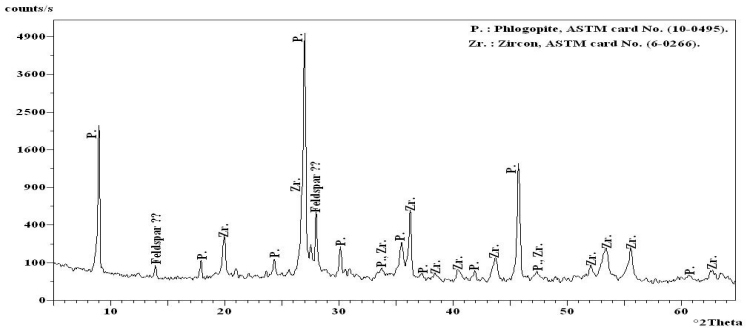

Fig. 30: X-ray diffraction pattern of zircon and phlogopite in the studied peraluminous pegmatites

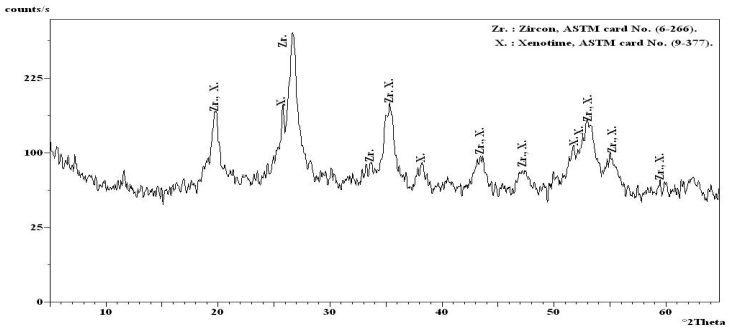

Fig. 31: X-ray diffraction pattern of zircon and xenotime in the studied peraluminous pegmatites

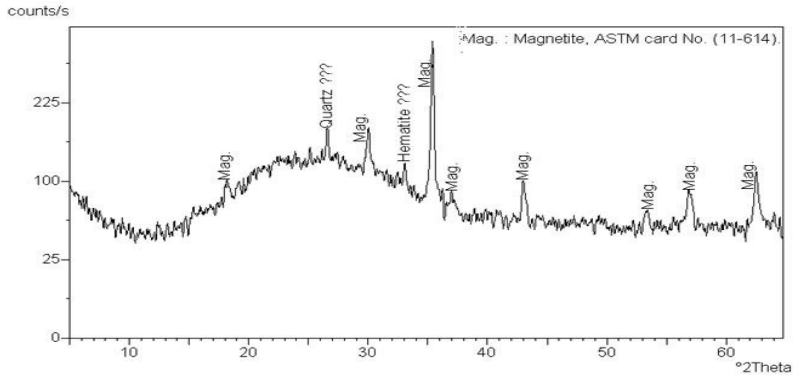

Fig. 32.: X-ray diffraction pattern of magnetite in the studied peraluminous pegmatites

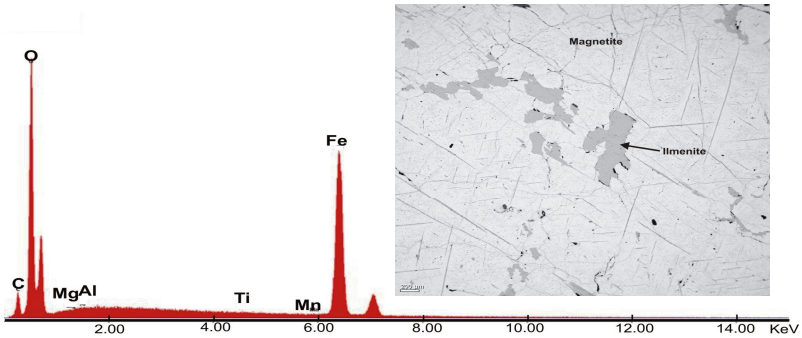

Fig. 33: ESEM backscattered data showing magnetite in the studied peraluminous pegmatites

91.74 % FeO, 0.3% MnO, 0.16% TiO_2 and 0.14 Al_2O_3.

Ilmenite ($FeTiO_3$)

Ilmenite occurs as accessory mineral in the studied peraluminous pegmatites associated with magnetite. It has an iron black or asphaltic colour as well as it is metallic with dull luster black streak and confirmed by ESEM (Fig. 34), it composed of 34.48 % FeO, 51.2% TiO_2, 16.39% MnO and 0.11 Al_2O_3.

MICROPROBE ANALYSIS OF MAGNETITE

Mineral compositions were determined on the JEOL JXA-733 Superprobe, operating conditions were 15 kv, with a beam current of 50 nA and peak counting time was 30 seconds for all elements at the Microscopy and Microanalyses Facility, University of New Brunswick (UNB), Fredericton, New Brunswick, Canada (Tables 3 to 7). The standards used are Hmt (for Fe), Ilm (for Ti), Grtpyr (for Al, Si, Mg), Bust (for Mn, Ca), Vmet (for V), Chr (for Cr), Comet (for Co), Gahnite (for Zn) and NiO (for Ni). Five magnetite grains were systematically selected named A, B, C, D and E. The five grains were chemically analyses by microprobe along profiles as seen in Figs. 35-39.

In the grain no. A; the magnetite is enrich in FeO, Al_2O_3, SiO_2, CoO and Cr_2O_3 (Table 3), whereas ilmenite in TiO_2, MnO, MgO, V_2O_3 and ZnO.

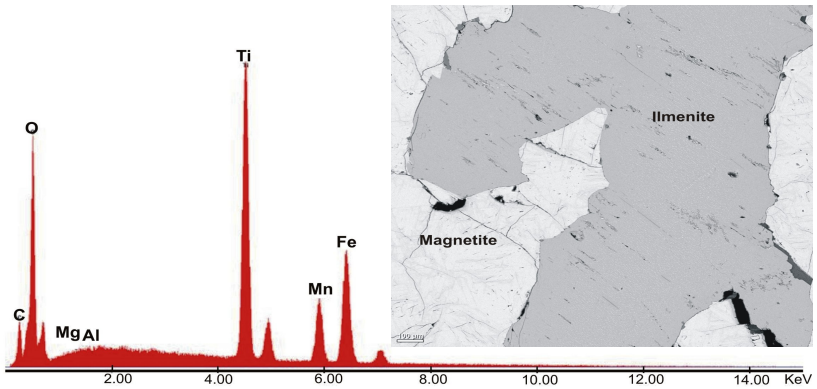

Fig. 34: ESEM backscattered data showing ilmenite in the studied peraluminous pegmatites

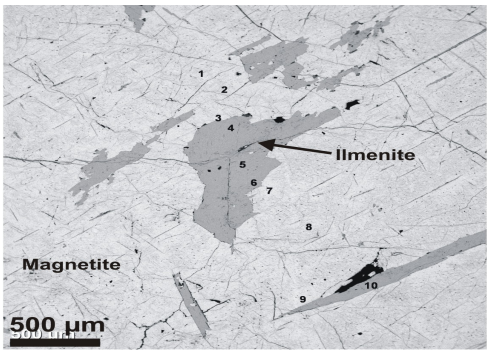

Fig. 35: Back-scattered- electron image showing profile of spots of microprobe analyses in magnetite grain no. A**,** Um Regeba area, south Eastern Desert

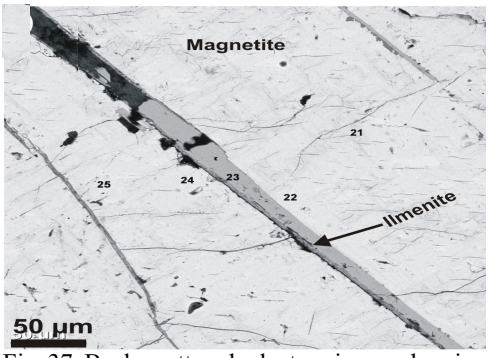

Fig. 37: Back-scattered- electron image showing profile of spots of microprobe analyses in magnetite grain no.C**,** Um Regeba area, south Eastern Desert

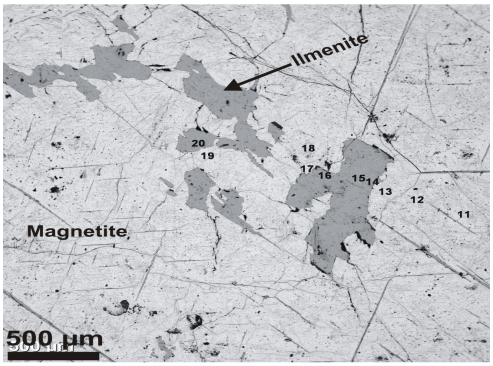

Fig. 36: Back-scattered-electron image showing profile of spots of microprobe analyses in magnetite grain no. B**,** Um Regeba area, south Eastern Desert

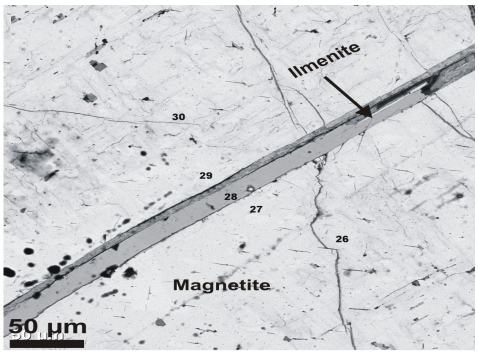

Fig. 38: Back-scattered- electron image showing profile of spots of microprobe analyses in magnetite grain no. D**,** Um Regeba area, south Eastern Desert

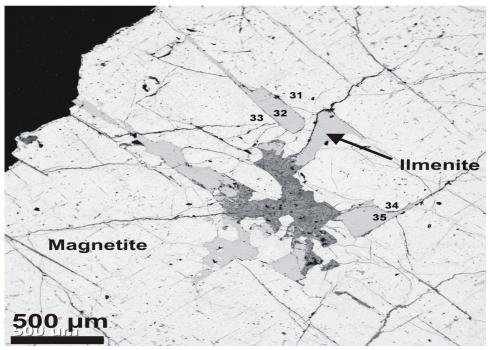

Fig.39: Back-scattered- electron image showing profile of spots of microprobe analyses in magnetite grain no. E, Um Regeba area, south Eastern Desert

In the grain no. B; the magnetite is enrich in FeO, Al_2O_3, SiO_2, MgO, CoO, V_2O_3 and Cr_2O_3 (Table 4), whereas ilmenite in TiO_2, MnO and ZnO (except spot no. 18).

In the grain no. C; the magnetite is enrich in FeO, Al_2O_3, SiO_2, MgO, CoO, V_2O_3 and Cr_2O_3 (Table 5), whereas ilmenite in TiO_2, MnO and ZnO.

In the grains no. D and E; the magnetite is enrich in FeO, Al_2O_3, SiO_2, MgO, CoO, and Cr_2O_3 (Tables 6 and 7), whereas ilmenite in TiO_2, MnO, V_2O_3 and ZnO.

In general the magnetite is enrich in FeO, Al_2O_3, SiO_2, CoO and Cr_2O_3 (Table 8), whereas ilmenite in TiO_2, MnO and ZnO. The values of V_2O_3 and MgO fluctuated from one grain to the other, where CaO and NiO contents are negligible.

SPECTROMETRIC INVESTIGATION

The instrument used in the ground γ-ray spectrometric survey measurements is RS-230. Ground γ-ray spectrometric survey can detect dose rate (D.R.) in unit ($nSvh^{-1}$), potassium (K%), equivalent uranium content (eUppm) and equivalent thorium content (eTh ppm). Uranium mobilization (eUm) in the studied rock types can be calculated as follows; the uranium mobilization is calculated by the difference between the measured eU and the expected original uranium, which is calculated by dividing the measured eTh by the average eTh/eU ratio in the crustal acidic rocks (original uranium = eTh/3.5 according

Table 3 : Microprobe analysis of magnetite grain no. A

Wt%	1	2	3	4	5	6	7	8	9	10
FeO	89.28	90.58	91.13	33.31	33.64	34.59	90.76	89.27	91.03	32.21
TiO_2	0.0698	0.03	0.4438	49.29	48.81	47.44	0.0608	0.0342	0.202	49.98
Al_2O_3	1.358	0.3471	0.2412	0.0129	0.0237	0.0264	0.341	0.2324	0.2242	0.9297
SiO_2	0.127	0.0435	0.0403	0.0082	0.0122	0.0134	0.038	0.1746	0.0391	0.0133
MnO	0.1115	0.1118	0.1548	15.42	15.64	14.9	0.1165	0.1776	0.1476	14.45
MgO	0.0066	0.0045	0	0.0085	0.0158	0.025	0	0.011	0.0047	0.0911
CaO	0	0	0	0	0	0	0	0.0059	0	0
V_2O_3	0.1154	0.1075	0.114	0.3128	0.3436	0.2146	0.1054	0.1123	0.1129	0.1375
Cr_2O_3	0.008	0.0061	0.0075	0	0	0	0.0015	0.0048	0.0066	0
CoO	0.0997	0.0943	0.1043	0.041	0.0384	0.0348	0.1044	0.0936	0.099	0.0394
ZnO	0	0.0015	0.0003	0.1264	0.1303	0.0968	0.0113	0.0196	0.0015	0.4365
NiO	0	0	0	0	0	0	0	0	0	0
Total	91.17	91.33	92.24	98.53	98.65	97.34	91.54	90.13	91.87	98.29

Table 4 : Microprobe analysis of magnetite sample no. B

Wt%	11	12	13	14	15	16	17	18	19	20
FeO	90.49	90.65	87.05	33.35	33.35	34.72	88.05	89.58	89.75	36.21
TiO_2	0.038	0.0496	0.0982	49.04	48.59	48.21	0.1951	0.0486	0.1141	47.7
Al_2O_3	0.24	0.312	0.2495	0.0192	0.0183	0.0217	0.3378	2.1811	0.3038	0.021
SiO2	0.0384	0.0482	0.259	0.0146	0.0151	0.0142	0.2206	0.0514	0.037	0.0184
MnO	0.1442	0.1433	0.1655	15.61	15.9	14.94	0.1155	0.1861	0.1507	13.63
MgO	0	0.0036	0.008	0.0084	0.0071	0.0082	0.0022	0.0792	0.0047	0.0313
CaO	0	0	0.0151	0	0.0005	0	0.0183	0	0	0
V_2O_3	0.1045	0.114	0.1053	0.1042	0.0787	0.1037	0.1052	0.112	0.1048	0.1319
Cr_2O_3	0.0081	0.005	0.01	0	0	0	0.0096	0.0013	0.0067	0
CoO	0.0933	0.0954	0.0946	0.0245	0.0292	0.0348	0.0939	0.0996	0.0912	0.04
ZnO	0.0075	0.0057	0.0184	0.1256	0.1147	0.0891	0.0219	0.3685	0.0082	0.1123
NiO	0	0	0	0	0	0	0	0	0	0
Total	91.16	91.42	88.08	98.31	98.11	98.14	89.17	92.71	90.58	97.89

Table 5: Microprobe analysis of magnetite grain no. C

Wt%	21	22	23	24	25
FeO	87.47	90.05	29.87	88.95	91.61
TiO_2	0.0658	0.3405	50.62	0.4456	0.0785
Al_2O_3	0.5566	0.2234	0.0317	0.3617	0.2733
SiO_2	0.2366	0.0436	0.0227	0.0465	0.04
MnO	0.1327	0.1263	17.44	0.1483	0.0862
MgO	0.0143	0.0013	0	0.0003	0.0033
CaO	0.0177	0	0	0	0.0006
V_2O_3	0.1201	0.11	0.0784	0.1183	0.1114
Cr_2O_3	0.0062	0.0105	0	0.0069	0.0107
CoO	0.0999	0.0965	0.0322	0.0926	0.1045
ZnO	0.1053	0.0235	0.2223	0.0009	0.0139
NiO	0	0	0.0023	0	0
Total	88.82	91.03	98.32	90.17	92.33

Table 6: Microprobe analysis of magnetite sample no. D

Wt%	26	27	28	29	30
FeO	91.7	90.97	29.65	89.2	91.1
TiO_2	0.076	0.1863	50.08	0.1862	0.0815
Al_2O_3	0.5489	0.2825	0.075	0.2904	0.2733
SiO_2	0.0597	0.0436	0.0322	0.1483	0.0438
MnO	0.1491	0.1556	17.91	0.1287	0.154
MgO	0.0237	0.0037	0.0028	0.0037	0.0075
CaO	0	0	0.0032	0.0082	0
V_2O_3	0.1067	0.1045	0.1905	0.1147	0.1093
Cr_2O_3	0.0046	0.0053	0	0.0079	0.0039
CoO	0.0981	0.1047	0.0217	0.0973	0.1031
ZnO	0.0197	0.0047	0.2236	0.0158	0.0045
NiO	0	0	0	0	0
Total	92.78	91.86	98.19	90.21	91.88

Table 7: Microprobe analysis of magnetite grain no. E

Wt%	31	32	33	34	35
FeO	90.9	35.71	92.01	92.27	33.08
TiO_2	0.0795	46.18	0.1535	0.0758	48.12
Al_2O_3	0.8104	0.0248	0.2851	0.278	0.0181
SiO_2	0.0503	0.0157	0.0317	0.0372	0.0177
MnO	0.1781	15.71	0.1497	0.1572	16.79
MgO	0.0284	0.0031	0.0021	0	0.005
CaO	0	0	0	0	0
V_2O_3	0.1143	0.1357	0.1138	0.1109	0.1345
Cr_2O_3	0.0078	0	0.001	0.0076	0
CoO	0.1105	0.0397	0.0969	0.1037	0.039
ZnO	0.1071	0.2015	0.0113	0.0193	0.1911
NiO	0	0	0	0	0
Total	92.39	98.02	92.85	93.06	98.4

to Clark et al., 1966) to give the leaching values of uranium (eUm= eU-eTh/3.5). Positive values indicate uranium addition by mobilization, whereas negative values indicated migration of uranium by leaching.

The eU contents in the studied peraluminous granites range between 0.6 and 3.20 ppm with an average of 1.96 ppm. The eTh contents range between 2.4 and 13.20 ppm with an average of 5.65 ppm, while the average of (eTh/eU) ratios are 3.32 ppm and (eU/eTh) ratios are 0.42, and average of eUm is 0.35 indicating its magmatic origin (Table 9 and Fig. 40). The eU contents in the studied peraluminous pegmatites range between 6.2 and 11.9 ppm with an average 9.12 ppm. The

Table 8: Average magnetite and ilmenite microprobe analyses of the five grains, Um Regeba area, south Eastern Desert, Egypt

Wt%	Grain A		Grain B		Grain C		Grain D		Grain E	
	Av. Mag.	Av. Ilm	Av. Mag.	Av. Ilm	Av. Mag.	Av. Ilm	Av. Mag.	Av. Ilm	Av. Mag.	Av. Ilm
FeO	90.34	33.44	89.26	34.41	89.52	29.87	90.74	29.65	91.73	34.4
TiO_2	0.1401	48.88	0.0906	48.39	0.2326	50.62	0.1325	50.08	0.1029	47.15
Al_2O_3	0.457	0.248	0.604	0.02005	0.3537	0.0317	0.3488	0.075	0.4578	0.0213
SiO_2	0.077	0.0118	0.1091	0.01558	0.09168	0.0227	0.07385	0.0322	0.0397	0.0167
MnO	0.1366	15.1	0.1509	15.02	0.0359	17.44	0.1469	17.91	0.1617	16.25
MgO	0.0045	0.0351	0.01628	0.01375	0.0048	0	0.0097	0.0028	0.0102	0.00405
CaO	0.00009	0	0.0056	0.000125	0.0037	0.0227	0.0021	0.0032	0	0
V_2O_3	0.1106	0.2521	0.1076	0.1046	0.115	0.0784	0.1088	0.1905	0.113	0.1351
Cr_2O_3	0.00575	0	0.0068	0	0.0086	0	0.0054	0	0.0055	0
CoO	0.0992	0.0384	0.09467	0.03213	0.09838	0.0322	0.1008	0.0217	0.1037	0.0394
ZnO	0.0057	0.1975	0.01195	0.1104	0.0359	0.2223	0.01118	0.2236	0.0459	0.1963
NiO	0	0	0	0	0	0.0023	0	0	0	0
Total	91.38	98.2	90.46	98.117	90.50	98.34	91.68	98.19	92.77	98.36

Mag.= Magnetite, Ilm.= Ilmenite

eTh contents range between 13.50 and 28.40 ppm with an average 21.76 ppm, while the average of (eTh/eU) ratios are 2.43 ppm and (eU/eTh) ratios are 0.42, and average of eUm is 2.95 indicating addition of uranium from surrounding rocks (Table 9 and Fig. 40).

The comparison between the radioelement concentrations in the peraluminous granites and peraluminous pegmatites at Um Regeba area relative to those of the crustal igneous rocks after IAEA (1979) and Boyle (1982) are listed in Table (9). It is noticed that the concentration of eU and eTh in the peraluminous granites at Um Regeba area are relatively lower than normal case as the corresponding values in the crustal average, whereas in the peraluminous pegmatites are higher than normal case as the corresponding values in the crustal average.

The binary relations of eU, eTh, and eTh/eU may provide an indicator of the geochemical behavior of U and Th in the studied rock samples. The plot of eU versus eTh (Fig. 41) illustrates that there have strong positive linear relation (r= 0.93) indicating their behavior

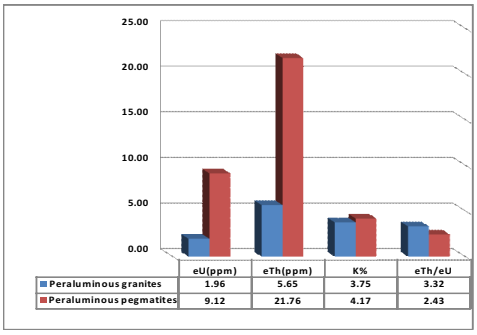

Fig. 40: A histogram for the average radiometric measurements of the Um Regeba peraluminous granites and peraluminous pegmatites

Table 9: The minimum, maximum and average of radiometric measurements of the Um Regeba peraluminous granites and peraluminous pegmatites, SED, Egypt.

		eU (ppm)	eTh (ppm)	K%	eTh/eU	eU/eTh	eUm
Peraluminous granites	Min.	0.6	2.40	1.70	0.81	0.094	-2.37
	Max.	3.20	13.20	6.70	10.67	1.24	2.39
	Aver.	1.96	5.65	3.75	3.32	0.42	0.35
Peraluminous pegmatites	Min.	6.20	13.50	3.0	1.80	0.28	-0.057
	Max.	11.90	28.40	5.40	3.53	0.55	4.80
	Aver.	9.12	21.76	4.17	2.43	0.42	2.90
Crustal acidic igneous rocks (after IAEA, 1979 and Boyle, 1982)							
Aver.		4.50	18	4	4	0.25	-

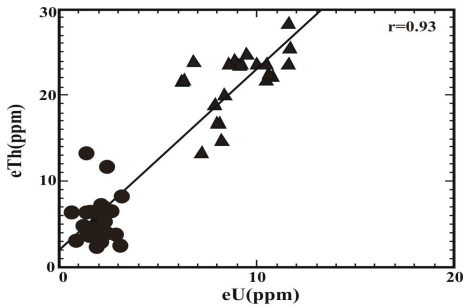

Fig. 41: eU vs. eTh variation diagram for the studied peraluminous granites and peraluminous pegmatites

was probably controlled by magmatic (Simpson et al., 1979). A poor negative relations (r= -0.10) exist between eTh and eTh/eU as shown on Fig. 42 indicating that uranium distribution in these rocks is not only controlled by magmatic processes but also by post-magmatic processes.

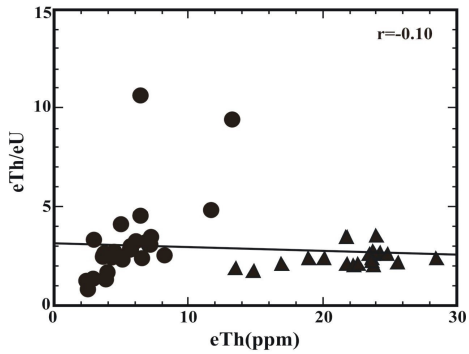

Fig. 42: eTh vs. eTh/eU variation diagram for the studied peraluminous granites and peraluminous pegmatites

CONCLUSIONS

The exposed rocks in the study area can be classified into the following litho-tectonic units: 1) psammitic gneiss, mostly quartz rich meta-psammites, meta-conglomerates and subordinate meta-pelites; 2) Migif-Hafafit gneisses and associated ultramafic and calc-alkaline igneous assemblages, granitoids and metasediments, generally medium metamorphic grade; 3) white gneissic granodiorite, trondhjemite, tonalite complex; 4) peraluminous granites and peraluminous pegmatites bearing magnetite; 5) late-orogenic granitoids (microgranite, felsite and aplite) (Greiling, 1990).

The peraluminous granites are emplaced into the older rocks of the area in a NNW-SSE trend-close to the major Nugrus thrust. The peraluminous granites are mainly composed of plagioclase (An_{5-10}), K-feldspar, quartz, biotite and muscovite. Allanite and zircon are common accessories.

The presence of cross-hatching (tartan pattern) as low-temperature transforming twinning in the studied peraluminous granites is consider as a product of a combination between albite and pericline twinning in peculiar relation. The chloritization and sericitization alteration are secondary textures in the granitic rocks arising from deuteric or later hydrothermal activity (Shelley, 1993).

The peraluminous pegmatites occur as pockets of variable dimensions vary from few centimeters to few meters in width and length, and mostly concordant with the common NW-trending of enclosing granites and other country rocks all over the area. The peraluminous pegmatites are coarse grained, composed essentially of K-feldspar, quartz, plagioclase (An_{6-10}), muscovite and biotite. Titanite, zircon, allanite and magnetite are common accessories.

Geochemically, the studied peraluminous granites and peraluminous pegmatites are monzogranite and syenogranite to alkali feldspar granite respectively. They have peraluminous character, calc alkaline and alkaline affinity respectively, emplaced in within plate setting, crystallized under water-vapor pressure (2-3 Kb) and temperature from 760° to 800°C, pertaining to the I-type granite originated by highly differentiated magma generated from upper mantle contaminated with some crustal materials. The studied peralu-

minous granite originated under high oxidation condition.

Mineralogically, the identified heavy minerals are classified into groups according to their anion either they are radioactive or non radioactive; 1- Silicate minerals (zircon & phlogopite), 2-Phosphate mineral (xenotime), 3-Oxide minerals (magnetite and ilmenite).

The magnetite mineralization was disseminated within the peraluminous pegmatites. The magnetite of Um Regeba area represents a late stage magmatic product. The pegmatite segregates magnetite crystals and form masses of magnetite, concentrated in response to fractional crystallization and this phenomenon is repeated in the peraluminous granites of W. El Gemal, especially in El Mokhattata area.

Magnetite showed lamellar intergrowth with ilmenite. Ilmenite is visible with a hand lens in most magnetite samples. The magnetite is enrich in FeO, Al_2O_3, SiO_2, CoO and Cr_2O_3, whereas ilmenite in TiO_2, MnO and ZnO. The values of V_2O_3 and MgO fluctuated from one sample to the other, where CaO and NiO contents are negligible. The enrichment of magnetite and ilmenite by the previous elements due to a geochemical behavior (ionic substitution). The depletion in CaO due to Ca^{+2} ions cannot substitute for Fe^{+2} in the magnetite and ilmenite lattice because it is considerably larger than Fe^{+2} and also differ in physical properties. The depletion in NiO is due to the magmatic origin of the magnetite.

Radiometrically, the radioactivity increases from the peraluminous granites to the peraluminous pegmatites. The average eU content in peraluminous granites is less than twice the Clark value (4 ppm). The average eTh/eU ratio is 3.32; indicating the rock is not uraniferous, while the average eU content in the peraluminous pegmatites is more than twice the Clark value (4 ppm) indicating the rock is uraniferous.

Acknowledgments

The authors would like to express their wishes to thank Prof. Dr. Gehad. M. Saleh for his help and reviewing the manuscript. The authors would also like to express their wishes to thank Prof. Dr. Mostafa Darwish for his kind help during the analysis of the studied samples.

REFERENCES

Ali, M.M.; Shalaby, M.H.; Osman, A.M., and Moharem, A.F., 1998. Comparative studies between the radioactivity of fresh and altered granites of Gabal Gattar, north Eastern Desert, Egypt. 4th Arab Conf. Peaceful uses of Atomic Energy, Tunis, A.H. Hashad (Ed.).

Aly, M.M., and Moustafa, M.M., 1984. Major chemistry statistics characterizing common igneous rocks of Egypt. 9th Inter. Cong. Stat. Comp. Sci. Res., Ain Shams Univ., Cairo.

Bai, T.B., and Van Groos, A.F.K., 1999. The distribution of Na, K, Rb, Sr, Al, Ge, Cu, W, Mo, La and Ce between granitic melts and coexisting aqueous fluids. Geochim. Cosmochim. Acta, 63, 1117-1131.

Batchelor, R.A., and Bowden, P., 1985. Proterozoic interpretation of granitoid rock series using multi-cationic parameters. Chem. Geol., 48, 43-55.

Boyle, R.W., 1982. Geochemical prospecting for thorium and uranium deposits. Develop. Economic, Geol., 16, El Sevier, Amsterdam, 489p.

Černý, P., and Meintzer, R.E., 1985. Fertile granites in the Archean and Proterozoic fields of rare-element pegmatites: Crustal environment, geochemistry and petrogenetic relationship. In: Recent advances in the geology of granite-related mineral deposits, (Taylor, R. P. and Strong, D. F. , Eds.). CIM, 39, 170-207.

Chappell, B.W., and White, A.J.R., 1974. Two contrasting granite types. Pacific Geol., 8, 173-174.

Clarke, M.B., 1981. The mineralogy of peraluminous granites. A review, Can. Contrib. Miner.

Petrol., 79, 3-17.

Clarke, S.P.Jr.; Peterman, Z.E., and Heier, K.S., 1966. Abundances in uranium, thorium and potassium. In: Handbook of physical constants. Geol. Soci. Amer., Memoir, 97, 521-541.

Clemens, J.D., and Wall, V.J.,1981. Crystallisation and origin of some peraluminous (S-type) granitic magmas. Can. Miner., 19, 111-32.

Dare, S.A.S.; Barnes, S.J.; Meric, J., and Neron, A., 2013. The use of trace elements in Fe-oxides as provenance and petrogenetic indicators in magmatic and hydrothermal environments. Mineral deposit research for a high-tech world. 12th SGA Biennial meeting. Proc. (1).

Debon, F.; Le Fort P.; Sheppard, S.M.F., and Sonet, J.,1986. The four plutonic belts of the Transhimalaya-Himalaya: a chemical mineralogical isotopic and chronological synthesis along a Tibet-Nepal section. J. Petrol, 27, 219-250.

Deer, W. A.; Howie, R. A., and Zussman, J., 1992. An introduction to the rock forming minerals. Longman group limited, England. Second edition.

De La Roche, H.; Leterrier, J.; Grandelaude, P., and Marchal, M.,1980. A classification of volcanic and plutonic rocks using R1-R2 diagram and major element analyses. Its relationships with current nomenclature. Chem., Geol., 29, 183-210.

Dingwell, D.B.; Hess, D.U., and Romano, C., 1998. Viscosity data for hydrous peraluminous granitic melts: comparison with the meta-aluminous model. Am. Mineral., 83, 236-239.

El-Kammar, A.; El-Aassy, I.E., and Abram, F. B., 1997a. Rare earth elements geochemistry and crystal chemistry of xenotime bearing sediments of Um Bogma area, Southwestern Sinai, Egypt. Chemie der Erde, 57, 91-101.

Fyfe, W.S.,1969. Some thoughts on granitic magmas, In: Mechanism of Igneous Intrusions (Newall, G., and Rast ,N., Eds.). Geol. J. Spec., Issue 2, 201- 216.

Greenberg, J. K.,1981. Characteristic and origin of Egyptian youngest granites. Summary Geol. Soc. Am. Bull., Part II, 92, 749 – 840.

Greiling, P.O., 1990. Wadi Hafafit Area–structural geology contribution by M.F. El Ramly.

Harris, N.B.W.; Pearce, J.A., and Tindle, A.G., 1986. Geochemical characteristics of collision zone magmatism. In: Collision Tectonics. Geological Society London (Coward, M. P., and Ries, A. C., Eds). Special Publication, 19, 67-81.

Holtz, F., and Barbey, P.,1991. Genesis of peraluminous granites II, Mineralogy and chemistry of the Tourem Complex 9 North Portugal, Sequential melting vs. restite unmixing, J. Petrol, 32, 959-978.

Inger, S., and Harris, N.,1993. Geochemical constraints on leucogranite magmatism in the Langtang Valley. Nepal Himalaya. J. Petrol, 34, 345-368.

International Atomic Energy Ageney, (IAEA), 1979. Gamma ray surveys in uranium exploration, Technical Report Series, paper no.186, 90,Vienna.

Imeokparia, E.G., 1981. Ba/Rb and Rb/Sr ratios as indicators of magmatic fractionation, postmagmatic alteration and mineralization Afu Younger Granite Complex, Northern Nigeria. Geochemical J., 15, 209 - 219.

Jolliff, B.L.; Papike, J.J., and Shearer, C.K., 1992. Petrogenetic relationships between pegmatite and granite based on geochemistry of muscovite in pegmatite wall zones, Black Hills, South Dakota,USA. Geochim. Cosm. Acta, 56, 1915-1939.

Keppler, H., and Wyllie, P.J.,1991. Partitioning of Cu, Sn, Mo, W, U and Th between melt and aqueous fluid in the systems haplogranite-H2O-HCl and Haplogranite-H2O-F. Contrib. Mineral. Petrol., 109, 139-150.

Keppler, H.,1993. Influence of fluorine on the enrichment of high field strength trace elements

in granitic rocks. Contrib. Mineral. Petrol., 114, 479-488.

Khomyakov, A.P. ,1970. Rare earth minerals as potential geothermometers. Dokl. Acad. Sci. U.S.S.S.R., Earth Sci. Sect., 191, 182-183.

Le Maitre, R.W., 1976. The chemical variability of some common igneous rocks. J. Petrol., 17, 589 – 637.

London, D.,1987. Internal differentiation of rare-element pegmatites effects of boron, phosphorus, and fluorine. Geochim Cosmochim. Aeta 51, 403-420.

Luth, W.C.; Jams, R.H., and Tuttle, O.F., 1964. The granite system at pressure of 4 to 10 kilobars. J. Geophys. Res., 69, 759-773.

Mahmoud, M., 2009. Highlight on the geology, geochemistry and spectrometry of the muscovite granites at Wadi El Gemal area, South Eastern Desert, Egypt, Ph.D. Thesis, Suez Canal Univ., Egypt, 227p.

Mohamed, F.H., and Hassanen, M.A.,1997. Geochemistry and petrogenesis of Sikait leucogranite, Egypt: an example of S-type granite in a metapelitic sequence. Geol. Rundsch, 86 , 81-92.

O'Connor, J. T., 1965. Classification of quartz-rich igneous rocks based on feldspar ratio, U.S. Geol. Surv. Prof. Paper 525-B, B-79, B-84.

Pearce, J.A.; Harris, N.B.W., and Tindle, A. G., 1984. Trace element discrimination diagrams for the tectonic interpretation of granitic rocks. J. Petrol., 25, 956-983.

Saleh, G.M., 1992. Geologic and radiometric studies on the basement rocks of G. Nasb Aluba, Southeastern Desert, Egypt. M. Sc. Thesis. El Mansoura Univ., 170 p.

Shalaby, M.H., 1995. New occurrence of uranium mineralizations G VII, Gabal Qattar uranium prospect, north Eastern Desert, Egypt. Bull. Fac. Alex. Univ., 35 , No. 2, 447-460.

Shelley, D.,1993. Igneous and metamorphic rocks under the microscope. Chapman and Hall, London.

Simpson, G.M.; Lee, J.H., and Zoubok, B., 1979. A rating scale for tardive dyskinesia. Psychophar-macology, 64, 171-179.

Sun, S.S., and McDonough, W.F., 1989. Chemical and isotopic systematic of oceanic basalts: implications for mantle composition and processes. In: Magmatism in ocean basins (Saunders, A. D., and Norry, M. J., Eds.). Geol. Soc. London. Spec. Pub., 42, 313-345.

Sylvester, P.,1989. Post collision alkaline granites. J. Geol., 97, 261-280.

Takla, M.A., and Nowier, A.M., 1980. Mineralogy and mineral chemistry of the ultramafic mass of El- Rubshi, E. D., Egypt. Neues Jahrb. Min. Abh., 140/1, 17-28.

Tuttle, O.F., and Bowen, N.L.,1958. Origin of granite in the light of experimental studies in the system Na Al Si3O8 –K Al Si_3O_8-SiO_2-H_2O. Geol. Soc. Am. Mem., 74, 153.

Weaver, B., and Tarney, J., 1984. Empirical approach to estimating the composition of the continental crust. Nature, 310, 575-57.

Webster, J.D., and Rebbert, C.R., 1998. Experimental- investigation of H2O and C1 solubilities in F-enriched silicate liquids: implications for volatile saturation of topaz rhyolite mamas. Contrib. Mineral Petrol., 132, 198-207.

جيولوجية وإشعاعية الجرانيت الفوق الالومينى والبجماتيت المصاحب الحاويين لتمعدن الماجنتيت في منطقة أم رقيبة، جنوب الصحراء الشرقية، مصر

فراج محمد خليل و محمد سالم قمر

يهدف هذا البحث الى دراسة الجرانيت الفوق الالومينى والبجماتيت المصاحب له الحاويين لتمعدن الماجنتيت فى منطقة ام رقيبة والتى تقع جنوب الصحراء الشرقية على بعد ٨٠كم جنوب غرب مدينة مرسى علم. ينتشر الماجنتيت فى صخور الجرانيت الفوق الالومينى والبجماتيت المصاحب له بوادى الجمال وتم اخذ منطقة ام رقيبة كحالة للدراسة. تتكون المنطقة من صخور البساميتيك نايس ، مجعف – حفافيت نايس وما يصاحبها من الصخور النارية الفوق قاعدية و الكلسقلوية والجرانيتات و الرواسب المتحولة تحول متوسط الدرجة ، معقدات الجرانودايويت النايسي الأبيض مع التروندجيميت و التونالايت، الجرانيت الفوق الالومينى و البجماتيت المصاحب (الدراسة الحالية)، ثم الجرانيتات مابعد التجبل والتي تشمل الجرانيت دقيق التحبب، الفلسيت و الأبليت.

أوضحت الدراسة الجيولوجية والبتروجرافية ان صخر الجرانيت الفوق الالومينى متوسط الى خشن الحبيبات ابيض اللون متداخل فى صخر الجرانودايورايت مع وجود حد فاصل, ويتكون من البلاجيوكليز, الفلسبار البوتاسى, الكوارتز, البيوتيت والمسكوفيت بالاضافة الى الالنيت و الزيركون كمعادن اضافية, بينما صخر البجماتيت عبارة عن أجسام تشبه القواطع ذات ابعاد مختلفة تتراوح من عدة سنتيميترات الى عدة مترات داخل صخر الجرانيت الفوق الالومينى ويتكون من الفلسبار البوتاسى, الكوارتز, البلاجيوكليز, المسكوفيت والبيوتيت بالاضافة الى التيتانايت, الزيركون, الالنيت و الماجنتيت كمعادن اضافية.

وتشير الدراسات الجيوكيميائية ان الجرانيت والبجماتيت الفوق الالومينى عبارة عن مونزوجرانيت (كلسى قلوى) وسيانوجرانيت الى جرانيت الفلسبار القلوى (قلوى) بالترتيب ذوالنوع (I) وتداخلت فى بيئة حيث مصدرها مواد الوشاح العلوى مع بعض مواد القشرة الارضية,وتداخلهما ارتبط ببيئة للتلاحم بين الألواح، حيث تم التبلور تحت ضغط منخفض الى متوسط (٢-٣ كيلو بار) وتحت درجة حرارة حول ٧٦٠- ٨٠٠ درجة سيليزية.

ومن خلال تحليل العينات باستخدام حيود الأشعة السينية والميكروسكوب الماسح الألكتروني تم الحصول على مجموعة من المعادن تم تقسيمها اعتمادا على الانيون الى: معادن سيليكات (الزريكون والفلوجوبيت), معادن الفوسفات (الزينوتيم), معادن الاكاسيد (الماجنتيت والالمنيت). بدراسة النشاط الإشعاعي في منطقة الدراسة تبين ان الإشعاع يزداد من الجرانيت الفوق الالومينى إلى البجماتيت,حيث الجرانيت الفوق الالومينى يصل متوسط محتواها من اليورانيوم إلى ١,٩٦ جزء في المليون والثوريوم الى ٥,٦٥ جزء فى المليون بينما في البجماتيت يصل متوسط محتواها من اليورانيوم الى ٩,١٢ جزء في المليون والثوريوم الى ٢١,٧٦ جزء في المليون.

وبدراسة الماجنتيت تحت الميكروسكوب الماسح الالكترونى وجد أنه مصاحب لمعدن الالمنيت, ومن خلال دراستهم بأستخدام الميكروبروب الالكترونى وجد الاتى: كلا من الماجنتيت والالمنيت غنيان بأكسيد الحديد,اكسيد التيتانيوم, اكسيد الالمنيوم, اكسيد السيليكون, اكسيد المنجنيز, اكسيد الكوبالت, اكسيد الكروم, اكسيد الفانديوم, اكسيد الزنك واكسيد المغنسيوم. ووجد ان الماجنتيت غنى فى أكسيد الحديد, اكسيد الالمنيوم, اكسيد السيليكون, اكسيد الكوبالت واكسيد الكروم, بينما الالمنيت غنى فى اكسيد التيتانيوم, اكسيد المنجنيز واكسيد الزنك. ووجد ان قيم اكسيد المغنسيوم و اكسيد الفانديوم تتغير من عينة الى اخرى. ووجد ان عملية اثراء المجانيتيت والالمنيت بهذة الاكاسيد يرجع الى السلوك الجيوكيميائى (الاستبدال الايونى). وجد ان تمعدن المجانيتيت ذو اصل مجماتى تكون فى مراحل متأخرة نتيجة التبلور الجزئى.